STATIC LOADING TESTS AND SIMULATION BASED ON FE ANALYSIS OF RC SHEAR WALLS WITH ENVELOPED OPENING

Y. Oikawa [1], M. Sakurai [2], T. Nishida [3]

[1] *Graduate Student, Graduate School of Akita Prefectural University, Japan, m21c003@akita-pu.ac.jp*
[2] *Assistant Professor, Akita Prefectural University, Japan, sakurai_masato@akita-pu.ac.jp*
[3] *Professor, Akita Prefectural University, Japan, tetsuya_nishida@akita-pu.ac.jp*
...

Abstract

The method of multiplying the reduction factor of an opening area by the shear strength of a reinforced concrete (RC) shear wall without an opening has been used in the shear estimation of RC shear walls with openings, and has also been adopted in the Architectural Institute of Japan (AIJ) design standard for RC structures in Japan. In particular, in the estimation of the shear walls with multiple openings, a method of replacing each opening with a single enveloped opening is also described. The enveloped opening is defined by the projected length and height of each opening. Although the opening layouts are different, the shear strength of shear walls with the same reduction factor value for the openings is calculated using the above method. However, experimental results of shear walls with different opening pitches in a previous experiment showed different shear strength values; there is a difference between the shear estimation method of the enveloped opening and the experiment.

In this study, static loading tests for RC shear walls with openings varied opening agreement were carried out to verify the current shear estimation of RC shear walls using enveloped openings. In the tests, the stress of the wall panels, in which the shear capacity is neglected by the application of the enveloped opening was measured using an original small stress meter embedded in the wall panel, and it was compared to the actual stress at the wall panel subjected to a seismic load with the application condition of the enveloped openings calculation method in RC shear walls. Furthermore, simulation for the loading tests was carried out based on FE analysis to investigate the stress transferring mechanism at the wall panel in derail.

The specimens are designed to simulate the lower two stories of multi-story shear wall in a medium-rise RC building and scaled to one-third of the prototype walls. The experimental variables investigated were the layouts of the openings. This shear strength estimation is similar with the AIJ design standard. Specimens WEO1 and WEO2 have two 200 mm × 300 mm and 300 mm × 300 mm openings and an opening pitch of 200 mm and 400 mm, respectively.

From the test results, in Specimen WEO1, shear slip occurred at the central wall panel in the 2nd story, followed by the occurrence of a shear crack at the central wall panel in the 1st story and wing wall in the 2nd story. In specimen WEO2, shear failure occurred at the central wall panel in the 1st and 2nd stories, then, a shear crack occurred at the wing walls in the 1st and 2nd stories. The calculated shear capacities of the specimens showed that all specimens were underestimated by the replacing method in the experiment, although the test results of Specimen WEO2 showed good agreement with the estimation. Moreover, the concrete stress in the shear wall measured using a stress meter showed that the shear capacity of the central wall panel did not contribute to the entire shear capacity in Specimen WEO1.

In FE analysis, the two specimens were modelled based on the method of previous study. The analytical simulations showed good agreement with the experimental results such as the hysteresis loops, failure progress, and so on.

Keywords: RC shear wall with openings, enveloped opening, static loading test, shear strength, FE analysis

1. Introduction

In general, reinforced concrete (RC) shear walls, which are used in many buildings, are one of the main elements of earthquake resistance. However, there are some cases in which openings are arranged in their design owing to design restrictions. In the shear estimation of RC shear walls with openings, a method that multiplies the reduction factor related to the openings by the shear strength of RC shear walls without openings has been adopted in the Architectural Institute of Japan (AIJ) design standard for RC structures in Japan [1]. In particular, in the estimation of shear walls with multiple openings, a method of replacing each opening with

2i-0158

a single enveloped opening is described to simplify the calculation. The enveloped opening is defined by the projected length and height of each opening. Although the opening layouts are different, the shear strength of the shear walls with the same reduction factor value for the openings is calculated using the above method. However, it has been clarified from past experiments [2] and earthquake damage that the shear strength differs according to the difference in opening pitch. It is considered that there is a difference between the shear estimation method of the enveloped opening and the experiment; however, the above method has not yet been verified by experiments.

In this study, static loading tests for RC shear walls with openings that have varied opening agreement is carried out to verify the current shear estimation of RC shear walls using the enveloped openings method. Furthermore, simulations of the loading tests were carried out based on FE analysis to investigate the stress transferring mechanism at the wall panel in detail.

2. Experimental Program

2.1 Outline of specimens

Details of the configuration and reinforcement of the specimens are shown in Fig. 1 and Table 1. The specimens are designed to simulate the lower two stories of a multi-story shear wall in a medium-rise RC building and scaled to one-third of the prototype walls. The specimens are designed to estimate the same maximum shear capacity based on AIJ standards, although the shape and pitch of the openings are different. Especially, each specimen with 400 mm height × 600 mm length openings is evaluated for maximum shear capacity by replacing multiple openings with a single enveloped opening using the AIJ method shown in Fig. 2. Each specimen has two openings. Specimens WEO1 and WEO2 have 200 mm height × 300 mm length, and 300 mm height ×300 mm length openings with an opening pitch of 200 mm and 400 mm, respectively. The material properties of the concrete and reinforcement are shown in Table 2.
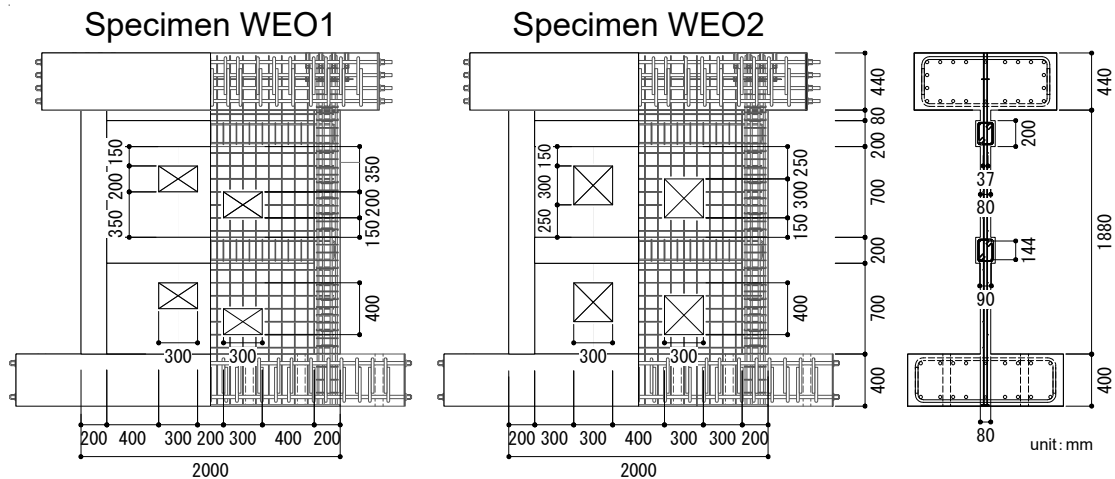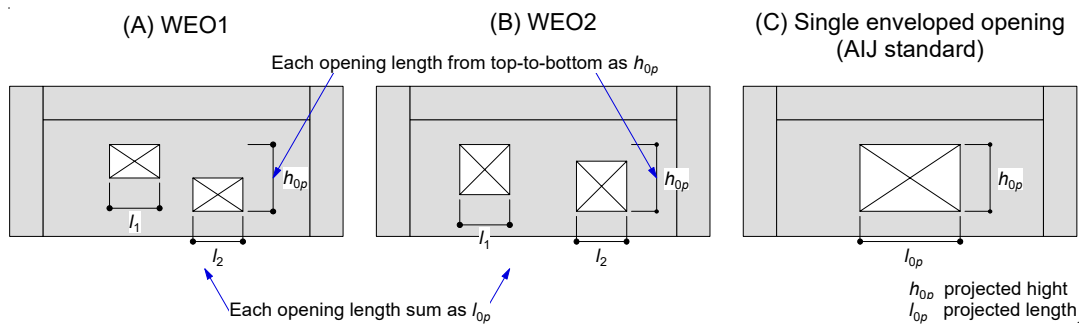

Fig. 1 – Test specimens

Fig. 2 – Replacing enveloped opening (AIJ standard)

2

Table 1 – Specification of section

Column	B×D (mm × mm)	200×200
	Longitudinal bar	12-D13 (Pg=3.8%)
	Tie	2-D6@60 (Pw=0.53%)
	Sub-tie	2-D6@120 (Pw=0.53%)
Beam	B×D (mm × mm)	150×200
	Longitudinal bar	4-D10 (Pg=3.8%)
	Stirrup	2-D6@100 (Pw=0.42%)
Wall	Thickness (mm)	80
	Longitudinal bar	D6@100 zigzag
	Transverse bar	D6@100 zigzag
	Opening reinforced bar	D10

Table 2 – Properties of material in experiment

Steel bar			
Type	Location	σ_B (N/mm^2)	Es (N/mm^2)
D6	Wall bar, Tie, Stirrup	418.5	2.06×10^5
D10	Beam/Opening reinforcement	361.5	1.86×10^5
D13	Column reinforcement	469.8	1.65×10^5
Concrete			
WEO1	1st story	30.2	3.01×10^4
	2nd story	30.3	3.00×10^4
WEO2	1st story	28.7	3.01×10^4
	2nd story	30.3	3.00×10^4

2.2 Loading method

The apparatus used for loading is shown in Fig. 3. The specimen was fixed to a strong floor using a PC steel bar, and cyclic lateral loading was applied to the upper stub by two horizontal jacks of 2000 kN capacity under a constant axial load (N/BDσ_B=0.16, N: axial load) by two vertical jacks of 500 kN capacity.

The loading was conducted by controlling the relative wall drift angle, R, given by the ratio of the height corresponding to the measuring point of the horizontal displacement at the top of the specimen from the 1st story wall leg, h (2100 mm), to the horizontal deformation, δ, i.e., R=δ/h. The experiment was controlled according to the loading cycle in Table 3, and the displacement between the drift angle R of 1/10000 rad. to R of 1/1250 rad. was defined as the initial deformation region.

Table 3 – Loading cycles in experiment

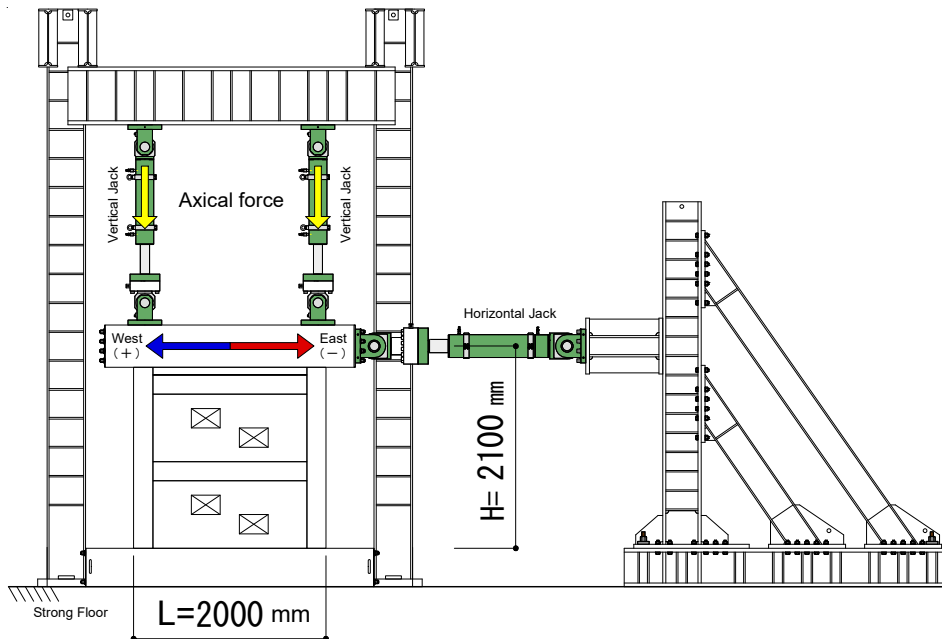| Drift angle (rad.)	Measure disp. (mm)	Cycle	Drift angle (rad.)	Measure disp. (mm)	Cycle
1/10000*	0.21	2	1/500	4.2	2
1/5000*	0.42	2	1/333	6.3	2
1/3333*	0.63	2	1/250	8.4	2
1/2500*	0.84	2	1/200	10.5	2
1/1667*	1.26	2	1/133	15.79	1
1/1250*	1.68	2	1/100	21.0	1
1/1000	2.1	2	1/67	31.34	1

* initial deformation region

Fig. 3 – Loading apparatus

2.3 Outline of stress measurement

Fig. 4 shows the image of the proposed sensor, and Fig. 5 shows its arrangement. This study uses a self-made stress meter developed by previous research as the proposed sensor with a 20 mm diameter and 60 mm height, which can be buried in concrete and can measure compressive stress up to approximately 30 MPa [3]. The stress measurement section of the steel is designed to be equivalent to the elastic modulus of concrete, and the stress is calculated from the strain of the constricted part partitioned by the acrylic plate. Because the proposed sensor mainly measures stress in the longitudinal direction, it is necessary to arrange it relative to the main axis of the strut formed on the wall plate in each loading direction. The mark in Fig. 5 indicates the mounting direction of the proposed sensor. The blue mark in the positive loading whereas the red mark in the negative loading. Both were attached to the reinforcement of the test specimen using steel wire to achieve a 45° angle from the horizontal.
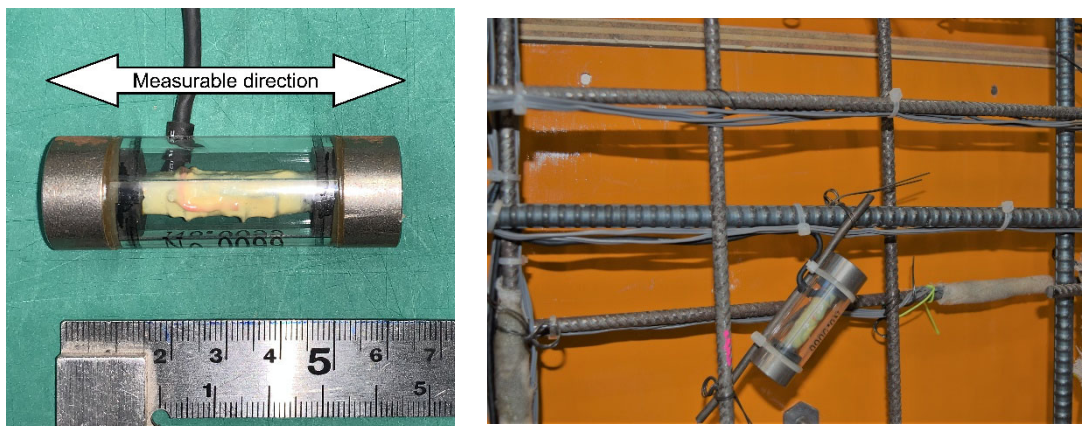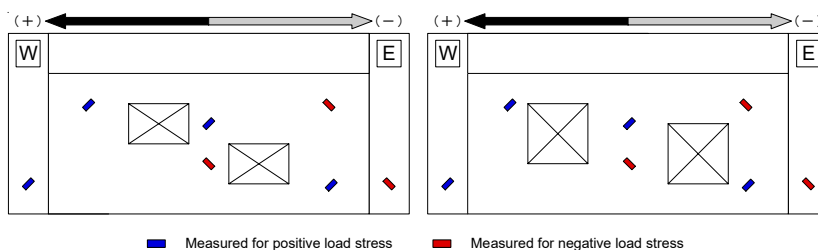

Fig. 4 – Image of the proposed sensor

4

Fig. 5 – Arrangement of proposed sensors in the 1st story

3. Experimental Results

3.1 Damage process and hysteresis loop

Fig. 6 shows the shear force versus drift angle relationship, and Fig. 7 shows the crack patterns formed after the loading cycle R of 1/250 rad. In the cracking diagram, the cracks that occurred in the positive loading are shown by the blue lines, and those in the negative loading are shown by the red lines.

Because the displacement in the out-of-plane direction could not be controlled in any of the specimens, the loading was completed in the R of 1/100 rad. loading cycle, for Specimen WEO1 and in R of + 1/67 rad. for Specimen WEO2.

In Specimen WEO1, the maximum shear force reached +567.5 kN at R of +1/250 rad., and -543 kN at R of -1/250 rad. At R of +1/250 rad., shear cracks of the central wall panel in the 2nd story increased significantly, and showed signs of compression failure. Slip failure and shear failure occurred in the central wall panel in the 2nd story at R of +1/200 rad., and R of -1/200 rad., respectively. The flaking and collapse of the concrete was then confirmed. In addition, indications of compression failure were observed at the wing wall beside the opening in the 2nd story and the central wall panel in the 1st story. After the R of 1/133 rad. loading cycle, compression failure occurred at the wing wall next to the opening in the 2nd story.

In Specimen WEO2, the maximum shear force reached +525.0 kN at R of +1/250 rad., and -473.5 kN at R of -1/250 rad. At R of 1/250 rad., small cracks of the central wall panel increased in the 1st and 2nd story, and the shear crack width of the central wall panel widened especially in the negative loading. In the R of +1/200 rad., shear cracks occurred in the central wall panel between the opening corners, and indications of flaking and compression failure at the opening corners and central wall panel also occurred. Shear failure as well as compression failure then occurred at each story of the central wall panel at R of -1/200 rad and R of +1/133 rad. Moreover, there was a compression failure at R of 100 rad. in the central wall panel wall and the west wing wall next to the openings on the 1st and 2nd stories.

Comparing Specimens WEO1 and WEO2, the slip fracture in the positive loading and shear fracture in the negative loading occurred in Specimen WEO1, and the fracture progressed mainly in the central wall panel on the 2nd story. On the other hand, shear fracture occurred in the central walls of the 1st and 2nd stories in Specimen WEO2, and an equal level of failure damage occurred in each story.
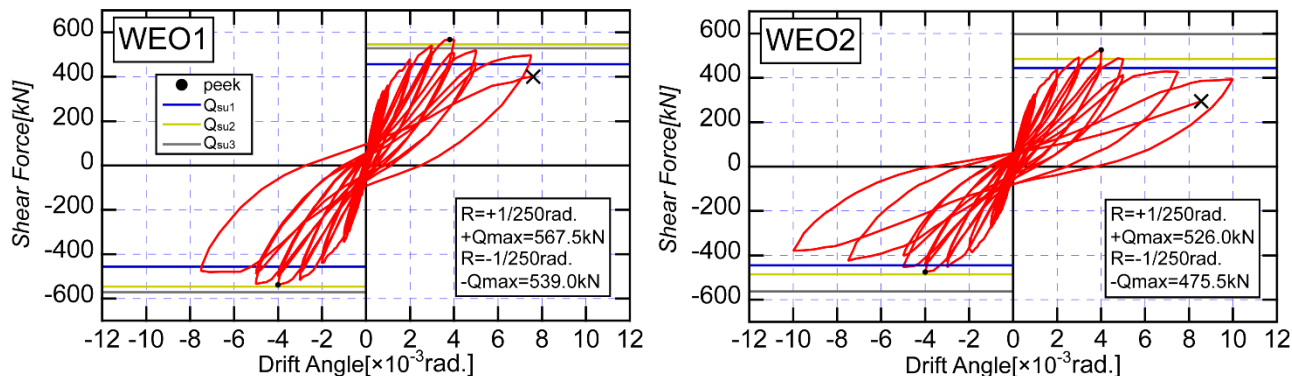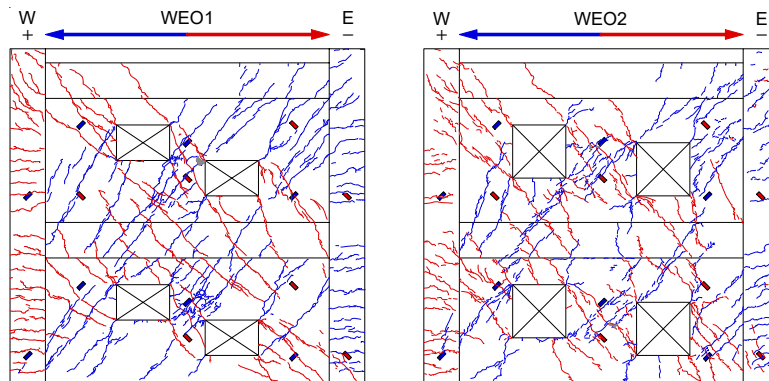

Fig. 6 – Shear force versus drift angle

5

Fig. 7 – Experimental cracking situation after the R=1/250 rad. loading cycle

3.2 Consideration of compressive stress in walls

Fig.8 shows the transition of each peak displacement of the loading cycle with respect to the stress at the measurement point of the wall panel in the 1st story. The figure shows the stress by the proposed sensor presented in the previous section and the stress in the principal stress direction by the triaxial strain gauge attached to the concrete surface at the same position. The proposed sensor is used to measure strut formation in the wall panel. However, because there is a possibility of a difference in the mounting direction of the proposed sensor and the principal stress direction, this section examines the difference between the mounting direction and the principal stress direction by comparing the stresses in the principal stress direction calculated from the triaxial strain gauge. In this figure, the positive side is referred to as tension and the negative side as compression. Furthermore, the graph on the left shows the results obtained up to the end of the experiment, and the graph on the right shows the results of the cycle up to R of 1/1000 rad. in the vicinity of the initial deformation region.

Comparing the stress of the proposed sensor with the minimum principal stress from the triaxial strain gauge, a stress divergence after R of 1/500 rad. was observed in all the measurement points. It is considered that the measurement results became unstable, because the triaxial strain gauge peeled off from the concrete surface as the cracks increased; the stress measurement of the triaxial strain gauge used in this experiment is difficult to use in places with large drift angles. The results were approximated by the stress from the proposed sensor and principal stress from the triaxial strain gauge at the east side opening lower part and in the central wall panel of Specimen WEO2, and the strut angle seemed to be approximately 45° when compared to the initial deformation. However, in the upper part of the west-side opening of Specimen WEO2 and the upper part of the east-side opening of both specimens, the increasing tendency of the compressive stress intensity remains constant although there is a difference in the stress intensity, suggesting that there is a deviation between the installation direction of the proposed sensor and the working principal stress direction. On the other hand, in the central wall panel of Specimen WEO1, it is inferred that the stress intensity was similar because the transition of the triaxial strain gauge was the same even though there was a large discrepancy between the results of the proposed sensor and the triaxial strain gauge in both loading directions.

In the comparison of the stress between the central wall panel and the wing wall, the east side wing wall, which is the compression side in the positive loading, showed higher stress than the other parts, and the shear force by the compression the wing wall seemed higher. According to the stress intensity obtained from the proposed sensor, the stress intensity of the central wall panel and the west wing wall in Specimen WEO1 was almost the same, and the shear capacity of the central wall panel seemed to be low because the area of the central wall panel was smaller than that of the wing wall. However, in Specimen WEO2, the stress transmitted to the central wall panel and east wing wall are the same, and the area is also same. Therefore, it is inferred that the shear force borne by each part is also the same. In the compression side wing wall, the stress increased with the displacement until the R of 1/133 rad.. On the other hand, the stress intensity of the central wall panel decreased after the R of 1/200 rad., and it was suggested that the central wall panel hardly contributed to the shear force, especially after the maximum strength. Moreover, comparing the stress in the positive and negative

6

loading, it is found that the gradual increase tendency of compressive stress with the progress of the loading cycle is smaller in the negative loading than in the positive loading. This is the reason the maximum shear capacity in the negative loading was lower than that in the positive loading.
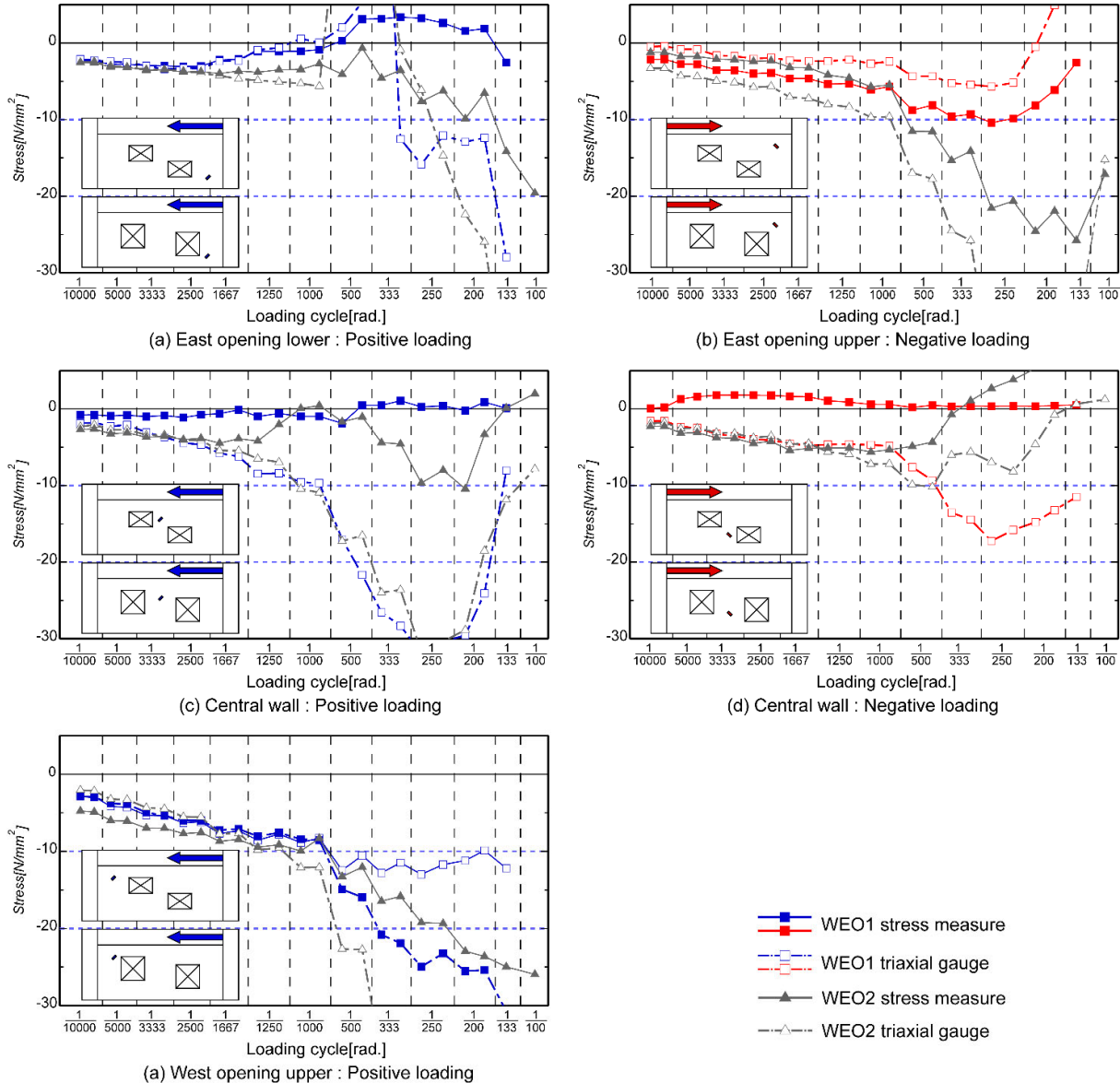

Fig. 8 – Stress and peak of loading cycles relationship with proposed sensors and triaxial strain gauges

3.3 Calculation of shear strength

The values of the calculated shear strength are listed in Table 4. In this section, the calculation results of Q_{su1} and Q_{su2} by Eq. 1 of [1] by AIJ standard, Q_{su3} by Eq. 4 of [4], the experimental results of Q_{exp}, and the ratio Q_{exp}/Q_{su} of each calculation are also listed in Table 4. The uniaxial compressive strength of the concrete used for the calculation was determined by the maximum strength of the story with the smaller value; the value of the 1st story was used. The calculation of the maximum flexural strength Q_{mu} is omitted, because it is confirmed that maximum shear strength becomes smaller than the maximum flexural strength, and it is a shear preceding fracture type. In the AIJ standard, the two opening reduction factors are calculated by the replacing method of the single envelope opening, and from the sum of the equivalent opening perimeter ratio. In the envelope opening method, Q_{su1} is calculated at the opening reduction ratio r_1, in the sum of the equivalent opening

perimeter ratio, and Q_{su2} is calculated at the opening reduction ratio r_2. The calculation results Qsu3 of the maximum shear strength are calculated by Eq. 4 and Eq. 5 based on the assumption of a compressed strut formed in the wall panel. The strut shape is assumed on the basis of [4] as shown in Fig. 9. For other symbols in the equations, see each reference.

$$Q_{sui} = r_i \left\{ \frac{0.068 p_{te}^{0.23}(F_c + 18)}{\sqrt{M/(Q \cdot D) + 0.12}} + 0.85\sqrt{\sigma_{wh} \cdot p_{wh}} + 0.1\sigma_0 \right\} t_e j_e \tag{1}$$

$$r_1 = 1 - max\left\{ 1.1 \times \frac{l_{0p}}{l}, 1.1\sqrt{\frac{h_{0p}l_{0p}}{hl}}, \frac{\sum h_0}{h} \right\} \tag{2}$$

$$r_2 = 1 - 1.1\sqrt{\frac{h_1 l_1 + h_2 l_2}{hl}} \tag{3}$$

$$Q_{wi} = v \cdot \cos\theta_i \cdot \sin\theta_i \cdot 0.5 l_{pi} \cdot t_i \tag{4}$$

$$Q_{su3} = \sum_{i=1}^{n+1} Q_{wi} \tag{5}$$

In the calculation results, the estimated Q_{su1} by the envelope opening replacing method was different from Q_{su2} and Q_{su3}, and the openings of Specimens WEO1 and WEO2 were evaluated equally; almost the same maximum shear capacity was estimated in both specimens. Q_{su3} was used to estimate the maximum shear capacity, which differed by the loading direction unlike other calculation methods.

In the calculation for Q_{su1}, Specimens WEO1 and WEO2 had results lower than the experimental results by 100 kN and 50 kN, respectively, and the experimental values were evaluated to be safe but were underestimated in the opening shape of Specimen WEO1. In the calculation for Q_{su2}, although the experimental results were overestimated by the negative loading of WEO2, the correspondence with the maximum shear capacity of the experiment was good in other results. In the case of Q_{su3} calculated by [4], the calculation accuracy was good, although it was assumed that there was no compressive strut in the central wall panel because of the opening arrangement not considered in [4] in the positive loading of Specimen WEO1. However, the calculation accuracy of the experiment was lower than that of others, and it was evaluated to be in danger. As shown in [4], the calculation accuracy of Eq. 5 tends to be low in the diagonal openings, and it is necessary to improve the accuracy for opening patterns like this opening arrangement.

Table 4 – Shear strength calculation

kN	Q_{exp}			Q_{su1}		Q_{su2}		Q_{su3}	
	Positive	Negative	Average	Reduction	Q_{su1}	Reduction	Q_{su2}	Positive	Negative
WEO1	567.5 kN	539.0 kN	553.3 kN	0.60	455.8 kN (1.21)	0.72	545.8 kN (1.01)	528.5 kN (1.07)	571.3 kN (0.94)
WEO2	526.0 kN	475.5 kN	500.8 kN	0.60	445.4 kN (1.12)	0.65	487.0 kN (1.03)	598.3 kN (0.88)	562.7 kN (0.85)

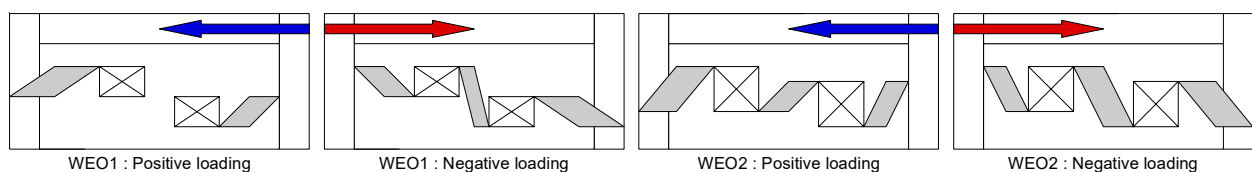*Calculation results of Q_{exp}/Q_{su} are shown in parentheses.

WEO1 : Positive loading　　WEO1 : Negative loading　　WEO2 : Positive loading　　WEO2 : Negative loading

Fig. 9 – Assumption of the compressive strut shape

8

2i-0158

4. Non-linear FE analysis

4.1 Analytical models

A two-dimensional non-liner FE analysis was also conducted for all specimens. The validity of the analysis model is examined to investigate the stress transfer mechanism of the RC shear wall with multiple openings. The finite element mesh layout for Specimen WEO1 is shown in Fig. 10. The concrete was modeled using quadrilateral elements, and the element mesh was a 50 mm × 50 mm wall; the column and beam were the element mesh along the main reinforcement bar. The reinforcing bar in the wall and transverse reinforcements of the columns and beams are substituted by equivalent layers with stiffness in the bar direction and superposed on the quadrilateral elements. The longitudinal reinforcement bars of the columns and beams were modeled by truss elements; the concrete and truss elements were bonded to reproduce the adhesion of the longitudinal bars. The FE non-linear analysis software "FINAL" was used in this analysis [6].
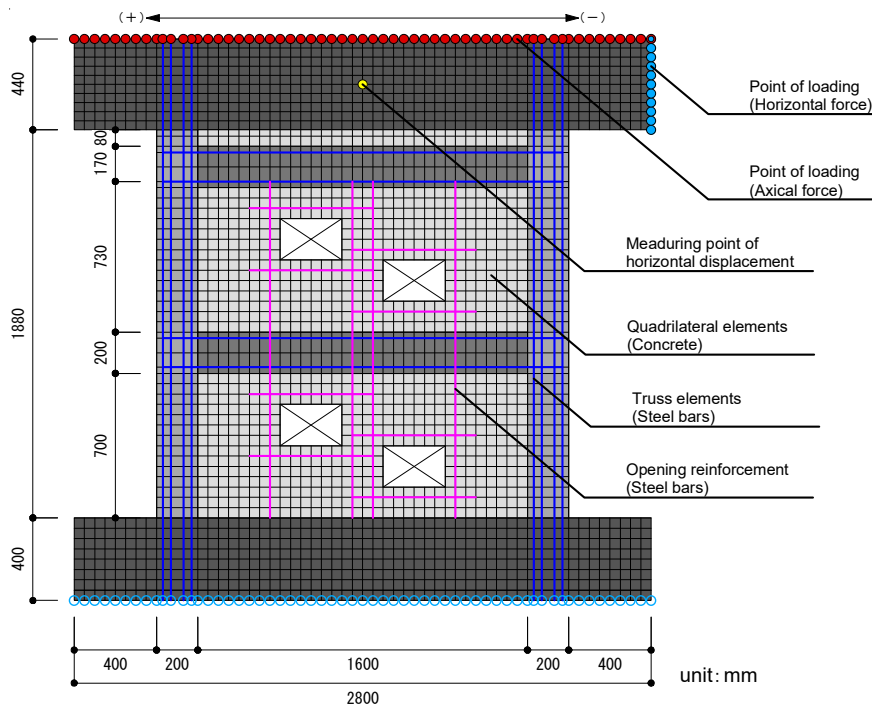

Fig. 10 – Finite element mesh

4.2 Element model

Table 3 shows the mechanical properties of the concrete used in the analysis. In this analytical model, the mechanical properties of reinforcing steel were used as the experimental values. For the concrete material, the tensile stress, elastic modulus and strain at compressive strength were calculated from the uniaxial compressive strength of the experimental values by the method described in [5], which considered the decrease in stiffness caused by minute crack accompanied with drying shrinkage, and the constitutive laws of the material was also following by [5]. Moreover, when the analysis of the initial deformation region is carried out, the maximum strength decreases by the stiffness degradation, and because the analysis is finished early by the increase of the unbalanced force in the convergence of the calculation, it is carried out according to the loading plan after the drift angle R of 1/1000 rad. in Table 3. The following equation was used to calculate the mechanical properties of concrete.

$$F_T = 0.5 \times 0.33\sqrt{\sigma_B} \tag{6}$$

$$E_C = 0.5 \times 0.3905{\sigma_B}^{0.556} \times 10^5 \tag{7}$$

$$\varepsilon_{C0} = 2 \times (13.7\sigma_B + 1690) \tag{8}$$

9

Table 3 – Mechanical properties used in the analysis

		σ_B (N/mm^2)	F_T (N/mm^2)		E_c (N/mm^2)		ε_{c0} (μ)	
			calculated	modified	experiment	modified	calculated	modified
WEO1	1st story	30.2	1.81	1.45	3.08×10^4	1.54×10^4	2104	4500
	2nd story	30.3	1.82	1.45	2.97×10^4	1.49×10^4	2105	
WEO2	1st story	28.7	1.77	1.41	3.08×10^4	1.54×10^4	2083	
	2nd story	30.3	1.82	1.45	2.97×10^4	1.49×10^4	2105	

4.3 Comparison of analysis with test

The shear force vs. drift angle relationships in the experiment and analysis are shown in Fig. 11. Comparing the hysteresis loop, the stiffness degradation in the positive loading appeared earlier than in the experiment in both analytical models, and there was a slight difference; however, the negative loading and the maximum strength showed almost equal values.

From the crack situation by the analysis shown in Fig. 12, it was found that the compression softening element tended to increase in the concrete at the same position in the analysis, while the collapse of the wall panel in the opening corner and central wall panel between the openings preceded in the experiment.

Thus, in the analysis, the failure in the 2nd story was concentrated in Specimen WEO1, and the failure level of each story was almost equivalent in Specimen WEO2. These results were similar in the experiment. These results indicate that the analysis can simulate the experimental results.

In the distribution of shear stress, compressive stress struts were formed in each wall panel of each analytical model. In both specimens, shear stress transfer was remarkable in the west wing wall, which was the compression side of each story in the positive loading; for the negative loading, the stress transferring was remarkable in the east wing wall, whereas the shear force transferred to the wing wall on the tension side was slight. In the shear transferring of the central wall panel, it is inferred that the stress transfer in the direction of the negative loading is small in all specimens, especially in the negative loading of Specimen WEO1, the stress transferring is hardly observed and does not contribute to the shear strength. In Specimen WEO2, the stress transmission in each member was remarkable, and the difference of the maximum shearing strength seemed to increase by the loading direction, because the stress transmission in the negative loading was small in each wall.
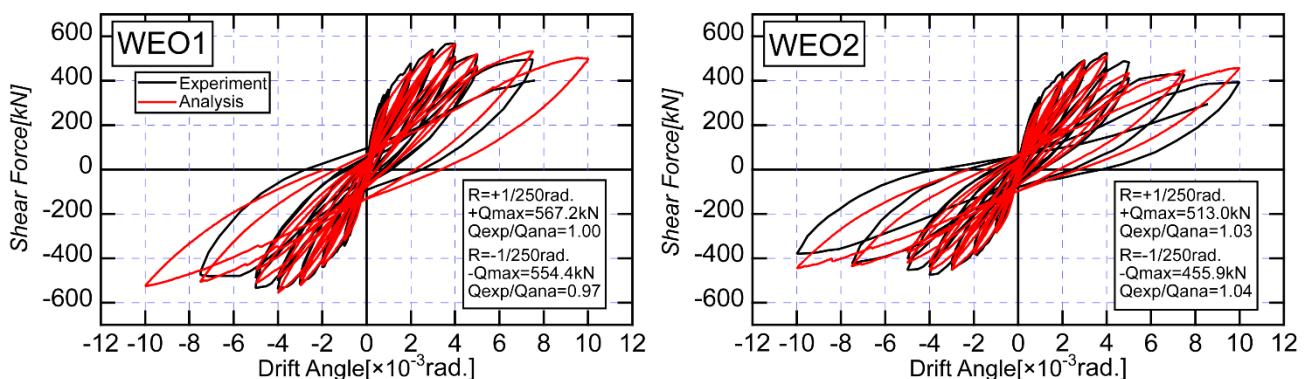

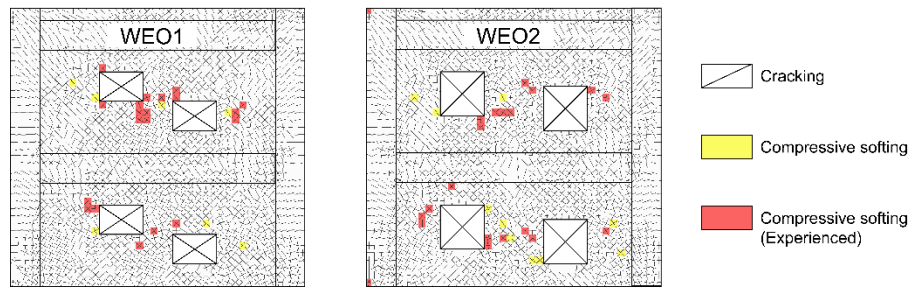Fig. 11 – Shear force versus drift angle (Comparison of the test and analysis)

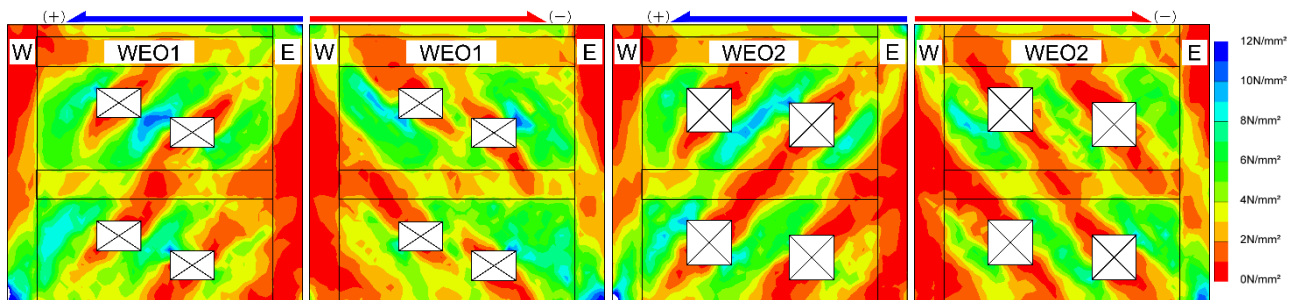Fig. 12 – Analytical Cracking situation after the loading cycle of R=1/250 rad.

Fig. 13 – Shear stress distribution of concrete element (R=1/250 rad.)

5. Conclusion

In this study, static loading tests of RC shear walls with multiple openings represented by Specimens WEO1 and WEO2 and their FE analysis were carried out to estimate the equivalent maximum shear capacity by making them single enveloped openings according to the AIJ standard. The results are as follows:

(1) In Specimen WEO1 with a narrow opening pitch, slip failure appeared at the central wall panel in the 2nd story. The collapse then proceeded to the central wall panel in the 1st story and the wing wall in the 2nd story. On the other hand, in Specimen WEO2 with a wide opening pitch, shear failure and collapse appeared at the central wall panel in each story, then the collapse proceeded to the wing wall in each story.

(2) In the comparison of the maximum shear capacity between the experimental results and the calculated shear strength, the results showed that Specimen WEO1 underestimated the experimental values, although the evaluation of the safety side was compared with the experimental value, when using the envelope opening method by the AIJ standard. In the meantime, the calculation results by the method based on the compressive strut was the opening arrangement, which was not assumed in the past literature; it is necessary to improve calculation accuracy for diagonal openings.

(3) From the analytical method proposed in this study, it was possible to reproduce the experimental results such as maximum shear strength and fracture property accurately.

(4) According to the contribution of the compressive stress in the wall panel, Specimen WEO1 showed the tendency that the stress was difficult to transmit in the central wall panel. In Specimen WEO2, the stress transfer in each wall panel between the openings was remarkable, and the stress transfer of each wall in the negative loading was smaller than that in the positive loading, especially. From the above, it is considered that the difference of the maximum shear strength according to the loading direction with the increase of the opening pitch affects the maximum shear strength.

Acknowledgements

References

[1] Architectural Institute of Japan. (2018): AIJ Standard of Structural Calculation of steel Reinforced Concrete Structures, Japan.

[2] Sakurai. M., KURAMOTO. H., Matsui. T. and Akita. T. (2008): Seismic Performance of RC Shear Walls with Multi-Openings, *Proceedings of 14th World Conference on Earthquake Engineering*, Paper-ID12-03-0071.

[3] Sakurai. M. (2017): Verification Test of Small Stress Sensors for Seismic Loading Tests with RC Member, *Web journal B of Akita Prefectural University*, Vol. 4, pp. 44-49, http://id.nii.ac.jp/1180/00000722/.

[4] Sakurai. M., Nishida. T. and Kobayashi. J. (2017): Effective of Opening Size on Compressive Strut of RC Shear Walls with Openings Based on FEM Analysis, *Proceedings of 16th World Conference on Earthquake Engineering*, Paper No.3771.

[5] Miura. S., Kobayashi. J., Sakurai. M., Tadokoro. M., Aizawa. N. (2017): FEM Analysis of RC Opened Shear Walls with Stress Concentration between Openings, *Proceedings of AIJ Tohoku Chapter Architectural Research Meeting,* No.80, pp.63-66. (in Japanese)

[6] ITOCHU Techno-Solutions Corporation (2011): FINAL/11 HELP.